energies

MDPI

Article

Design of Cement–Slag Concrete Composition for 3D Printing

Leonid Dvorkin [1,*], Vitaliy Marchuk [1], Izabela Hager [2] and Marcin Maroszek [2]

[1] Department of Constructing Products Technology and Material Science, Institute of Civil Engineering and Architecture, National University of Water and Environmental Engineering, 33000 Rivne, Ukraine; v.v.marchuk@nuwm.edu.ua

[2] Department of Building Materials Engineering, Faculty of Civil Engineering, Krakow University of Technology, 31-155 Krakow, Poland; izabela.hager@pk.edu.pl (I.H.); marcin.maroszek@doktorant.pk.edu.pl (M.M.)

* Correspondence: l.i.dvorkin@nuwm.edu

Abstract: The article presents a set of experimental-static models of the properties of fine-grained concretes on a cement–slag binder and quartz sand with the addition of a hardening accelerator made on a 3D printer. The influence of the factors of the composition of the mixture and the effects of their interaction on the studied properties of concrete was established. By analyzing the models, the influence of the factors of mixture composition on the studied properties was ranked. The nature and degree of interrelation of individual properties of concrete are shown. A method for calculating the optimal compositions of concrete for a 3D printer, providing the specified properties at a minimum cost, is proposed.

Keywords: Portland cement; concrete; granulated blast furnace slag; 3D construction printer; mathematical experiment planning; hardening accelerator additive

Citation: Dvorkin, L.; Marchuk, V.; Hager, I.; Maroszek, M. Design of Cement–Slag Concrete Composition for 3D Printing. *Energies* **2022**, *15*, 4610. https://doi.org/10.3390/en15134610

Academic Editor: F. Pacheco Torgal

Received: 29 April 2022
Accepted: 9 June 2022
Published: 23 June 2022

1. Introduction

At the present stage of construction development in Europe, the introduction of resource-saving technologies while ensuring high-quality building materials and structures is relevant. Structures based on Portland cement, which in turn is the most energy-intensive component of concrete and mortar, are widely used in construction, so it is advisable to develop technologies that significantly reduce its usage while maintaining or improving the quality of concrete and mortar. One such direction is the wide application in construction practice of composite cements, in which a significant part of the clinker is replaced by active mineral additives of man-made origin, in particular blast furnace granulated slag [1]. Additionally, an effective way to reduce the consumption of Portland cement in concrete and regulate its construction and technical properties is the introduction of such highly active mineral additives as microsilica, metakaolin and others. [2]. Modern construction is characterized by the increasing usage of new-generation concretes and mortars. In particular, such materials include concretes for additive technologies.

3D printers allow using extrusion molding of structures to provide high-speed robotic construction of objects, including complex shapes, with minimized consumption of materials and labor [3–5].

Most often, fine-grained concrete mixtures with the required strength, frost resistance, high adhesion and cohesion properties and curing speed are used for this purpose [6].

At present, a number of developments have been carried out in which mixtures are recommended, taking into account the characteristics of 3D printers and structures built with their use Table 1 [7].

Table 1. Recommended building mixes for 3D printing.

No.	Developer	Materials	Density, kg/m^3	Strength MPa		Technology Benefits	Technology Disadvantages
				In Splitting	In Compression		
1	Win Sun (China)	Cement–sand mixture with demolition waste, fiberglass and special additives	2000–2200	8.2	34.5	Used products of processing building materials, micro-reinforcement	Requires large production areas and maintenance personnel, the presence of non-functional formwork
2	AMT-SPETSAVIA (Russia)	High-strength cement–sandy fiber reinforced	2200–2350	–	от 30	Micro-reinforcement, material variability	The presence of non-functional formwork, uneven vertical surface
3	Stroy Bot (3D Printer)	Geopolymer concrete with puzzolan admixtures	2100–2250	–	–	Use of local raw materials for concrete mixtures	Uneven vertical surface
4	Bet-Abram (Slovenia)	Shotcrete with sand (0–4 mm) and gravel (4–8 mm) aggregates	2300–2350	–	–	The presence of anti-shrink additives	Non-functional formwork
5	Contour Crafting Corp. (USA)	Cement mortar for formwork, concrete for structures	2250	–	45–50	Leveled vertical surface, reinforcement	Low strength between layers
6	Apis Cor (Russia)	Fine-grained fiber reinforced concrete	2050	–	27.4	Micro-reinforcement	Uneven vertical surface, height limit 3.3 m
7	Loughborough University (Geat Britain)	Cement concrete	2250–2350	12–13	100–110	High strength, reinforcement structures.	Uneven vertical surface
8	CyBe Construction (The Netherlands)	Cement concrete	2200	6	45	Leveled vertical surface, fast setting and hardening of layers.	Unsynchronized mix feed and printer head movement
9	Batiprint 3D (France)	Polyurethane formwork filled with concrete	30	–	0.16	The formwork performs a heat-insulating function	Uncontrolled geometric parameters of structures, uneven vertical surface that needs protection from external influences
10	MIT Media Lab (USA)	Polyurethane formwork filled with concrete	–	–	–	The mobility of the extruder, the formwork performs the thermal insulation function of structures	
11	DUS Architects (The Netherlands)	Recycled plastic for formwork, lightweight concrete	–	–	–	Used secondary raw materials	The duration of the formwork manufacturing process

In the composition of mixtures along with fine sand, it is proposed to add aggregate up to 8–10 mm [8]. The mixtures may also include some types of wastes, for example, from the demolition and reconstruction of buildings and the recycling of construction materials [9]. Most concrete mixes include steel or non-metal fibers, setting regulators and other chemical additives.

The actual problem in the design of concrete mixes is to provide a set of necessary material properties while using available man-made raw materials. Currently, there are no universal solutions for the selection of construction mixes for 3D printers. In all cases, they must ensure normal extrusion of the mixture by the printer's printhead, the necessary structural strength sufficient for laying the subsequent layers, and the adhesive strength for reliable bonding of the layers to each other. As a result of curing, the mixture should achieve the necessary design parameters established for concrete [2].

The lack of the necessary regulatory database and insufficient development of the methodology for assigning the necessary indicators of the properties of mixtures and their testing significantly complicate the selection of concrete compositions for the 3D printer [2,10–12].

Since 2017, there has been a noticeable increase in the number of publications on 3D concrete printing material [13]; nevertheless, there is still a lack of standardized solutions to determine universal indicators of mixture parameters.

For additive manufacturing of building elements, it is important to use suitable materials that are low-energy-intensive and thus have a lower carbon footprint [14].

It remains a topical direction of using in additive technology such an active mineral additive in cement mixtures as granulated blast-furnace slag, produced in large quantities by the metallurgical industry [15,16]. As many studies and practical experience have shown, this material remains one of the most effective in composition with Portland cement.

Blast-furnace slag not only interacts with calcium hydroxide and promotes the formation of an additional amount of hydrosilicates in the cement stone, it also increases the carbonization coefficient of cement concretes and mortars, which has a positive environmental impact on the environment [17,18].

The use of rational concrete compositions, including, as a rule, mineral and organic additives, helps to reduce the consumption of cement clinker and, accordingly, carbon dioxide emissions during its production.

Compositions of building mixtures including granulated blast-furnace slag and providing a set of necessary properties for 3D printing cannot be considered sufficiently developed.

The aim of this work was to determine the effect of the composition of fine-grained concrete for 3D printing on a cement–slag binder and to propose a methodology for its design. The main tasks of the work were to obtain mathematical models of the properties of fine-grained concrete based on cement–slag binder and, on their basis, analyze the effects of technological factors. The tasks of the work were also to develop, with the help of the obtained models, a methodology for the computational design of optimal concrete compositions with desired properties at the lowest possible cost.

2. Materials and Methods of Research

Concrete mixes for 3D printer should provide their necessary formability during extrusion from the printer's head to achieve a given strength of layers (structural strength), as well as the adhesion ability of concrete with an acceptable setting time of the mixture without cracks and other defects.

In order to study the properties of extruded mixtures, a laboratory printer was designed and constructed as shown in Figure 1.

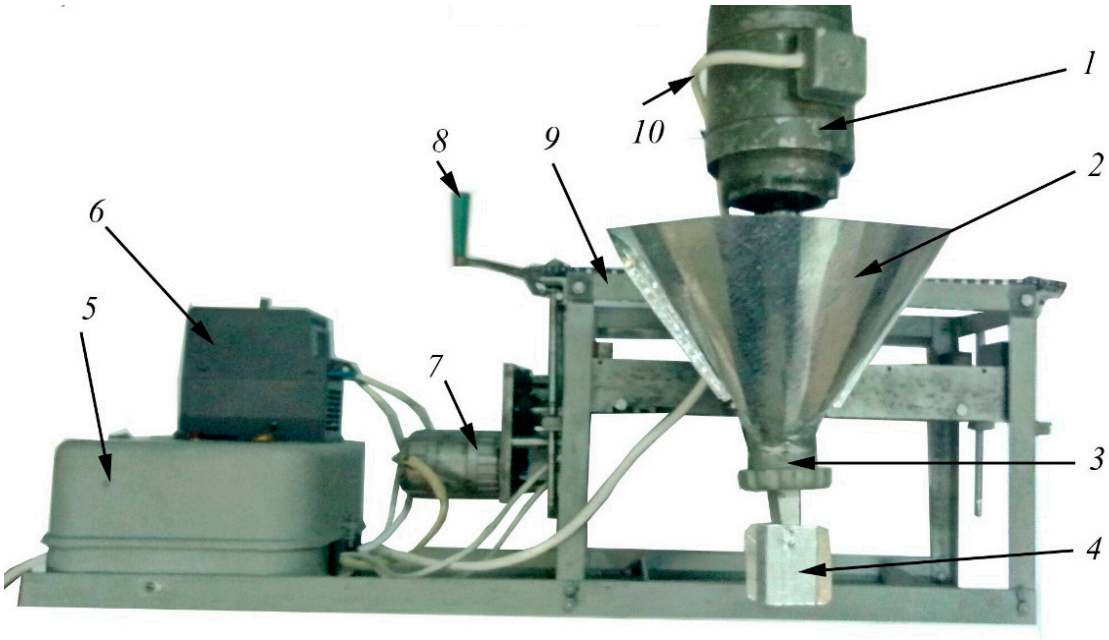

Figure 1. Laboratory 3D printer. 1—electric motor of the extruder; 2—hopper of building mixture; 3—auger; 4—mouthpiece; 5—control panel; 6—frequency converter of electricity; 7—reverse motor moving the extruder in the horizontal direction; 8—manual drive moving the extruder in the vertical direction; 9—frame; 10—power cable of electric motors.

Currently, there is no standardized method for determining structural strength. For its determination, a special device is proposed, which is shown in Figures 2 and 3 to measure the maximum specific load on a sample of extruded concrete layer at which it is beginning to deform.

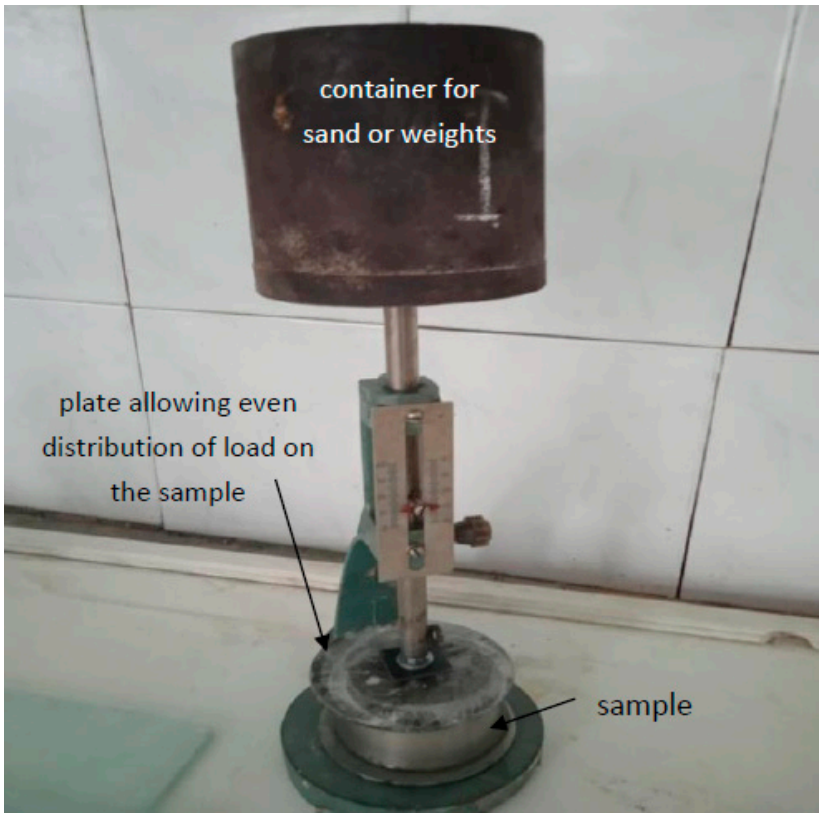

Figure 2. Device for determining the structural strength.

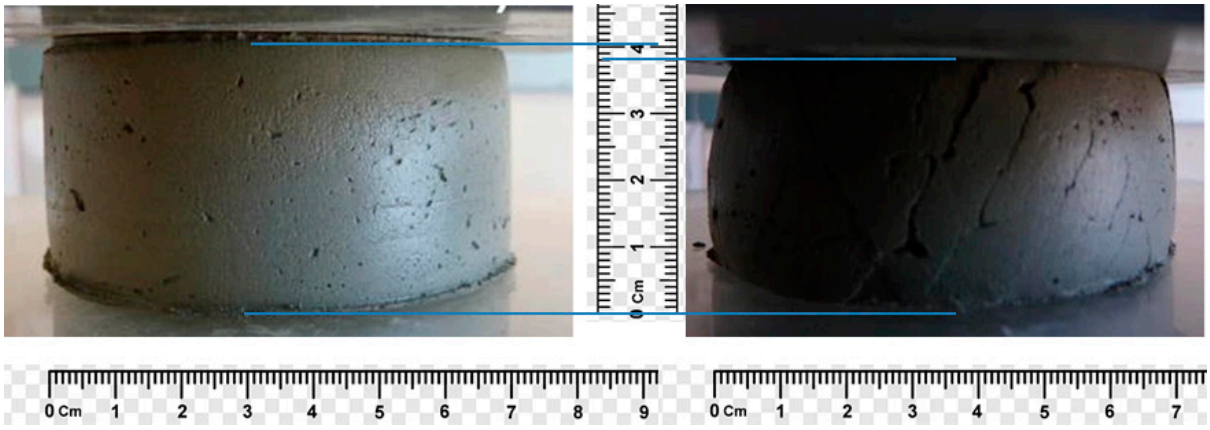

(**a**) (**b**)

Figure 3. An example of determining the structural strength of extruded concrete, (**a**) the sample withstands the load (structural strength is provided), (**b**) the sample is destroyed.

To obtain the mixtures, the used materials were Portland cement CEM I 42,5R (EN 197-1), ground-granulated blast-furnace slag. Quartz sand with fineness modulus 2.1 was used as an aggregate. The hardening accelerator Na_2SO_4 and the naphthalene-formaldehyde superplasticizer SP-1 were added to the mixtures. Preliminary experiments on a laboratory printer found that the optimal content of superplasticizer is 0.3% of the mass of cement–slag binder. A further increase in its content leads to a decrease in the structural strength of the mixture and, accordingly, the need to increase the duration of layer-by-layer molding. The chemical composition of Portland cement and granulated blast-furnace slag are given in Table 2. The mineralogical composition of the clinker was as follows: C_3S—57.10%; C_2S—21.27%; C_3A—6.87%; C_4AF—12.19% (EN 196-2). The specific surface area of Portland cement was S = 300–320 m^2/kg (EN 196-6).

Table 2. Chemical composition of raw materials *.

Name Material	L.O.I.	Oxide Content, %								
		SiO_2	Al_2O_3	Fe_2O_3	CaO	MgO	SO_3	K_2O	Na_2O	TiO_2
Clinker	-	21.80	5.32	4.11	66.80	0.95	0.63	0.54	0.42	-
Blast-furnace slag	0.59	39.51	6.47	0.14	47.19	3.12	1.76	-		0.25

* The chemical composition of Portland cement based on the used clinker was distinguished by an additional SO_3 content due to the introduction of gypsum in the amount of 3.1%.

The quality factor of blast-furnace granulated slag is determined by the ratio:

$$K_a = \frac{CaO + Al_2O_3}{SiO_2 + TiO_2}$$

It fluctuates for slag of most cereals at metallurgical enterprises in the range of 1.2 . . . 1.7. The used slag according to the value of K_a, which determines the hydraulic activity, can be considered ordinary. For this, the value of K_a = 1.35.

The content of the glass phase in the slag was 75–80%, its specific surface S = 320–350 m^2/kg EN 196-6, density—2.9 g/cm^3, bulk density—1340 kg/m^3, intergranular voidness—45.9%, intragranular porosity—15.5%.

The concrete mixture for testing was produced in two stages. In the first stage, in accordance with the conditions for planning experiments, a dry mixture was made by

mixing cement, ground slag, hardening accelerator, and sand. Sand consumption (S) was found from the condition of absolute volumes

$$S = \left(1000 - \left(\frac{Cem}{\rho_c} + \frac{GBFS}{\rho_{GBFS}}\right)\right) \cdot \rho_s$$

where Cem, GBFS—amount of cement and slag, kg/m^3, ρ_c, ρ_{GBFS}, ρ_s—cement, slag and sand densities, respectively.

At the second stage, the resulting dry mixture was mixed with water until the required formability was obtained. The setting time of the resulting mixture was determined according to EN 196-3. The cleavage strength of the samples molded on a laboratory 3D printer was determined by measuring the force applied at the boundary of the layers necessary for their destruction. The compressive strength of the specimens was tested in accordance with EN 196-1.

3. Results and Discussion

In order to select the optimal parameters of the mixture composition, algorithmic experiments were performed in accordance with the typical plan B_3 [19]. Plan B_3 is a statistically valid three-level plan of experiments that provides for the need to test 17 series of samples while varying the studied factors within the established range, with the subsequent calculation of the coefficients of the regression equations for the studied parameters and a statistical assessment of their adequacy. The planning conditions for the experiments are given in Table 3.

Table 3. Experiment planning conditions.

Technological Factors		Levels of Variation			Variation Interval
natural view	coded view	−1	0	+1	data
Content of granulated blast furnace slag in the binder mixture (GBFS), %	X_1	50	40	30	−10
Na_2SO_4 hardening accelerator additive content (HA), % of the binder mass	X_2	0	1	2	1
Cement–slag binder content, kg/m^3, (Bnd)	X_3	300	400	500	100

The water consumption was varied to achieve the required workability by the standard cone slump method (8–10 cm), ensuring sufficient formability (extrusiveness) of the mixture. The suitability of mixtures for molding was determined by the time from the moment of mixing to the beginning of setting, at which it becomes impossible to further mold by the 3D printer.

After the processing and statistical analysis [19] of the experimental data given in Table 4, the regression equations which are shown in Table 5 were obtained, which can be regarded as mathematical models of the properties of the extruded concrete mixture and concrete on its basis.

Mathematical models allow quantitatively estimating the influence of varying factors (Figures 4 and 5), taking into account their possible interaction, on the studied properties, and to arrange them according to the degree of influence:

Setting time	HA > Bnd > GBFS
Structural strength after 10 min of curing	Bnd > HA > GBFS
Structural strength after 25 min of curing	HA > Bnd > GBFS
Structural strength after 40 min of curing	HA > Bnd > GBFS
Compressive strength at the age of 3 days	Bnd > GBFS > HA
Splitting tensile strength at the age of 28 days	Bnd > GBFS >> HA
Compressive strength at the age of 28 days	Bnd > GBFS >> HA

Table 4. Experimental research results.

No.	Setting Time, min	Structural Strength after Mixing and Hardening, Pa			Tensile Splitting Strength, MPa		Compressive Strength, MPa	
		10 min	25 min	40 min	3 days	28 days	3 days	28 days
1	35	5320	8513	15,160	6.6	9.3	19.7	32.7
2	60	3780	5679	10,700	4.5	6.7	10.8	21.2
3	85	3916	5482	9225	5.7	8.1	16.9	27.6
4	145	2730	4096	7000	3.9	6.1	7.8	19.5
5	70	4600	6916	12,300	4.9	6.6	13.8	19.4
6	95	3356	5034	9125	4.1	5	8.8	13.4
7	120	3426	5139	7480	4.4	6.1	13.1	17.1
8	160	2521	3781	6545	3.5	4.8	7.8	9.4
9	55	3637	5455	9375	4.3	7.7	12.9	21.7
10	85	3177	4765	7710	3.6	5.1	10.6	16.4
11	50	4020	6030	11,230	4.7	6.5	12	20.5
12	120	2900	4350	6970	4.0	6.5	12.7	18.5
13	50	4002	6003	9880	6.3	8.7	17.8	28.5
14	95	2782	4173	7180	4.2	5.2	9.4	13.0
15	65	3275	4913	8240	5.0	7.2	10.9	21.7
16	70	3300	4950	8260	4.7	6.9	10.6	21.4
17	65	3310	4965	8200	4.9	7.1	10.8	21.6

Table 5. Mathematical models of the properties of extruded concrete mixture and concrete.

Parameters Studied	Mathematical Models	
Setting time, min	$T = 66.4 - 15.0x_1 - 32.0x_2 - 19.5x_3 + 4.1x_1^2 + 19.1x_2^2 + 6.6x_3^2 - 2.5x_1x_2 - 2.5x_1x_3 + 6.3x_2x_3$	(1)
Structural strength after 10 min of curing, Pa	$P^{10}{}_m = 3295 + 230x_1 + 558x_2 + 610x_3 + 124x_1^2 + 177x_2^2 + + 108x_3^2 + 55x_1x_2 + 72x_1x_3 + 87x_2x_3$	(2)
Structural strength after 25 min of curing, Pa	$P^{25}{}_m = 4938 + 359x_1 + 932x_2 + 193x_3 + 273x_1^2 + 171x_2^2\ x_3^2 + \cdot 198x_1x_2 \cdot + 123x_1x_3 + 247x_2x_3$	(3)
Structural strength after 40 min of curing, Pa	$P^{40}{}_m = 8258 + 830x_1 + 2130x_2 + 1350x_3 + 296x_1^2 + 853x_2^2 + 283x_3^2 + 280x_1x_2 + 322x_1x_3 + 560x_2x_3$	(4)
Compressive strength at the age of 3 days, MPa	$f^3{}_{cm} = 11.66 + 1.4x_1 + 0.68x_2 + 3.67x_3 - 0.54x_1^2 + 0.06x_2^2 + 1.31x_3^2 + 0.51x_1x_2 + 0.96x_1x_3 - 0.06x_2x_3$	(5)
Splitting tensile strength at the age of 28 days, MPa	$f^{28}{}_{tn} = 6.89 + 1.03x_1 + 0.25x_2 + 1.1x_3 - 0.328x_1^2 - 0.228x_2^2 + + 0.222x_3^2 + 0.138x_1x_2 + 0.213x_1x_3 + 0.113x_2x_3$	(6)
Compressive strength at the age of 28 days, MPa	$f^{28}{}_{cm} = 20.74 + 4.7x_1 + 1.51x_2 + 4.88x_3 - 1.01x_1^2 - - 0.56x_2^2 + 0.69x_3^2 + 0.06x_1x_2 + 0.74x_1x_3 + 0.21x_2x_3$	(7)

The structural strength of mixtures for 3D concreting based on blast-furnace granulated slag (GBFS) increases with increasing amount of binder, the minimum proportion of GBFS in the binder (30%) and the use of the maximum amount, within the composition's research hardening-accelerator additive (Figure 4). It should be noted that a more significant effect of the accelerator additive is observed also when the proportion of GBFS in the binder is minimal.

The analysis of the models (Table 5) shows that in the range of variation in the studied factors the compressive strength of 3D-printing concrete containing GBFS and hardening accelerator additive varies within 9.4–32.7 MPa.

According to the obtained graphic dependences (Figure 5) with decreasing the proportion of GBFS from 50% to 40% of the binder and a gradual increase in the content of the binder from 300 kg/m^3 to 500 kg/m^3, it is observed an increase in compressive strength by 35–40% at the content of GBFS 40–50% and by 15–20% at the minimum slag content.

The figures show that the effect of hardening accelerator addition is also positive, which is more significantly manifested at the maximum binder content.

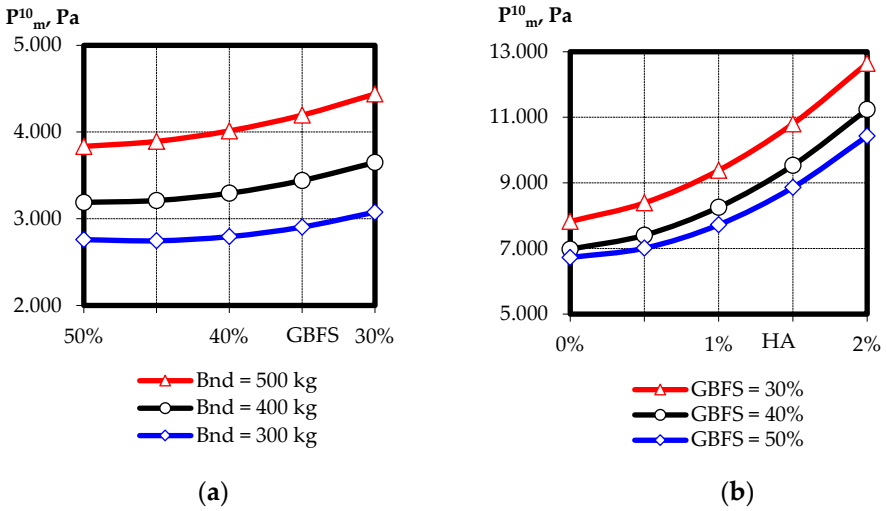

Figure 4. Graphical dependences of structural strength after 10 min (**a**) and 40 min (**b**) of mixture curing.

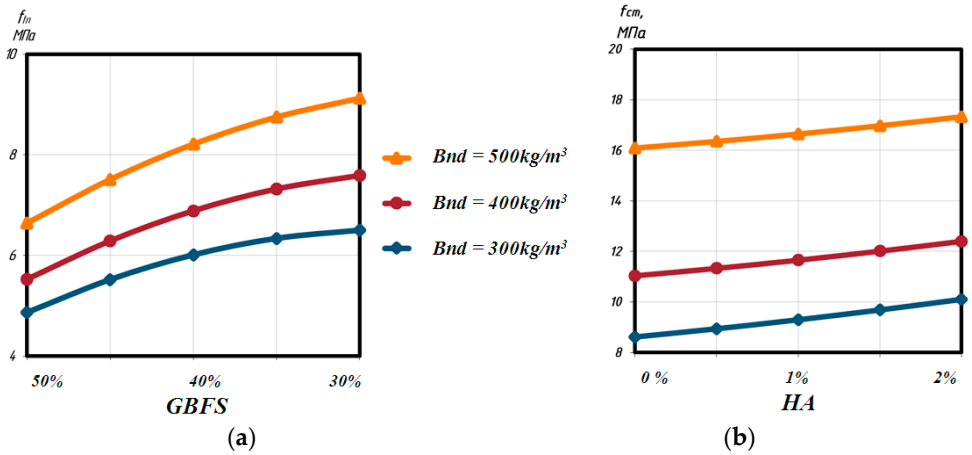

Figure 5. Graphical dependences of the compressive strength of concrete mixtures at the age of 3 days (**a**) and 28 days (**b**).

A joint analysis of the obtained mathematical models made it possible to establish their relationship Figures 6 and 7.

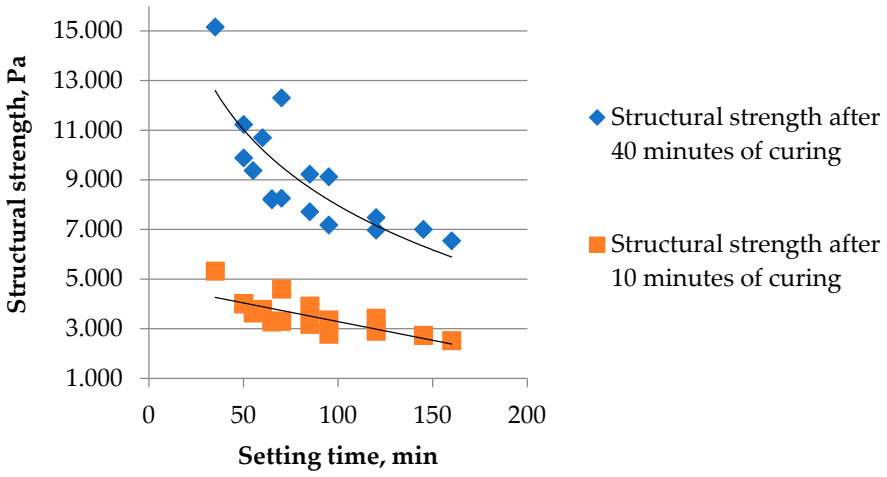

Figure 6. Relationship between setting time and structural strength of concrete.

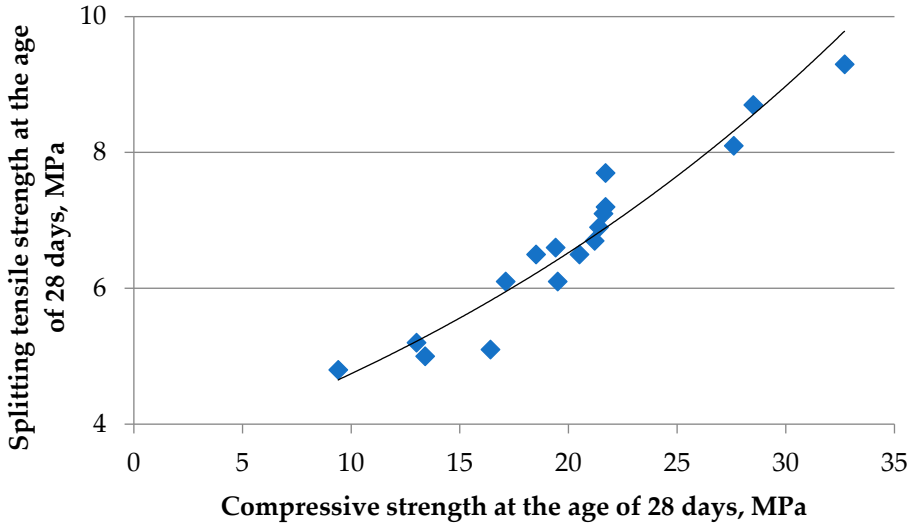

Figure 7. Relationships of tensile strength when splitting to compressive strength at the age of 28 days.

The complex of obtained models allows designing compositions of concrete mixtures intended for 3D printing, allowing obtaining the specified indicators of their properties.

When selecting the criterion of the minimum cost of the concrete mixture, the formulation of the problem can be formulated in general terms as follows: determine the values of the factors of the mixture composition $x_1 \ldots x_n$, allowing to minimize its cost while ensuring the specified parameters.

In the general case for the cement–slag fine-grained concrete mixture:

$$Ct_{cm} = Ct_{cem} \cdot Cem + Ct_{GBFS} \cdot GBFS + Ct_{Ad} \cdot Ad + Ct_S \cdot S \rightarrow \min \quad (8)$$

subject to

$$\begin{gathered} P_1 \geq f(x_1, x_2, \ldots, x_n); \\ P_2 \geq f(x_1, x_2, \ldots, x_n); \\ \ldots \\ P_m \geq f(x_1, x_2, \ldots, x_n) \\ \text{at } x_1 \ldots x_n \in [a \ldots b], \end{gathered} \quad (9)$$

where

Ct_{cm}, Ct_{cem}, Ct_{GBFS}, Ct_{Ad}, Ct_S—cost of the concrete mixture, cement, blast-furnace granulated slag, chemical additives and sand, respectively, USD/kg;
Cem, GBFS, Ad, S—amount of cement, slag, chemical additives and sand, kg/m^3;
$P_1 \ldots P_m$—specified quality indicators of the mixture and concrete based on it;
$x_1 \ldots x_n$—factors of the mixture composition considered in the models;
a, b—limits on the possible values of the factors.

Converting of the values of the mixture composition parameters normalized in this study (Table 5) in the coded form for model calculations is carried out according to the following dependences:

$$x_1 = \frac{GBFS - 40}{-10}; \; x_2 = \frac{HA - 1}{1}; \; x_3 = \frac{Bnd - 400}{100}. \quad (10)$$

The values of the fine aggregate (sand) consumption are obtained by the equation:

$$S = \left(1000 - \left(\frac{C}{\rho_c} + \frac{GBFS}{\rho_{GBFS}} + \frac{Bnd}{\rho_{Bnd}}\right)\right) \cdot \rho s \quad (11)$$

where ρ_c, ρ_{GBFS}, ρ_{Bnd}, and ρ_s—cement, slag, water and sand densities, respectively, for the materials used in the study ρ_c = 3.1 g/cm^3, ρ_{GBFS} = 2.9 g/cm^3, ρ_{Bnd} = 1.0 g/cm^3, and ρ_s = 2.65 g/cm^3.

The most rational way to solve such a problem is to use the software environment Microsoft Excel, in particular its application "Search for a solution" [20].

For the given values of properties and the content of components at certain restrictions on the values of the factors (in coded values from −1 to +1), the computer program goes through the possible combinations of factors and determines them in parallel to achieve the minimum cost of the mixture water consumption necessary to ensure the required workability of the mixture by the appropriate equation of regression. The values of water consumption (L/m^3) were found along with other output parameters in the process of performing experiments according to the selected plan.

$$W = 225 + 5x_1 - 4x_2 + 13x_3 + 2x_1^2 - 8x_2^2 - 4x_3^2 - 1x_1x_3 + 1x_2x_3 \quad (12)$$

Example

Determine the composition of cement–slag fine-grained concrete mixture for the 3D printer with a compressive strength of 3 and 28 days, respectively; 10 MPa and 20 MPa; splitting tensile strength at 28 days—5 MPa; and the beginning of setting at 45 min and the structural strength in 10 min and 40 min after mixing of 4150 Pa and 7000 Pa, respectively. The characteristics of the materials used are given above.

Take the cost of the main components of the mixture for the 3D printer as follows, USD/kg: Ct_{cem} = 0.28; Ct_{GBFS} = 0.02; $Ct_{Ad,HA}$ = 2; $Ct_{Ad,SP}$ = 3.2; Ct_A = 0.01.

1. Using experimental–statistical models (1)–(7) and substituting values of normalized parameters into them, the functions of restrictions (9) are obtained:

Setting time, min

$$66.4 - 15.0x_1 - 32.0x_2 - 19.5x_3 + 4.1x_1^2 + 19.1x_2^2 + 6.6x_3^2 - 2.5x_1x_2 - 2.5x_1x_3 + 6.3x_2x_3 = 45$$

10 min of curing, Pa

$$3295 + 230x_1 + 558x_2 + 610x_3 + 124x_1^2 + 177x_2^2 + 108x_3^2 + 55x_1x_2 + 72x_1x_3 + 87x_2x_3 \geq 4150$$

Structural strength after 25 min of curing, Pa

$$8258 + 830x_1 + 2130x_2 + 1350x_3 + 296x_1^2 + 853x_2^2 + 283x_3^2 + 280x_1x_2 + 322x_1x_3 + 560x_2x_3 \geq 7000$$

Compressive strength at the age of 3 days, MPa

$$11.66 + 1.4x_1 + 0.68x_2 + 3.67x_3 - 0.54x_1^2 + 0.06x_2^2 + 1.31x_3^2 + 0.51x_1x_2 + 0.96x_1x_3 - 0.06x_2x_3 \geq 10$$

Splitting tensile strength at the age of 28 days, MPa

$$6.89 + 1.03x_1 + 0.25x_2 + 1.1x_3 - 0.328x_1^2 - 0.228x_2^2 + 0.222x_3^2 + 0.138x_1x_2 + 0.213x_1x_3 + 0.113x_2x_3 \geq 5$$

Compressive strength at 28 days, MPa

$$20.74 + 4.7x_1 + 1.51x_2 + 4.88x_3 - 1.006x_1^2 - 0.556x_2^2 + 0.694x_3^2 + 0.063x_1x_2 + 0.738x_1x_3 + 0.213x_2x_3 \geq 20$$

2. In Equation (8), substitute the value of the cost of the components of the mixture, and set the limit values of the factors: from −1 to 1 (in coded form).
3. Using the "Search for a solution" software application, determine the values of the factors that satisfy the accepted constraints of the problem, and minimize the total cost of the mixture:

$$x_1 = 0.62; x_2 = 0; x_3 = 0.9.$$

At these values of factors according to Equations (1)–(7), T = 45 min and $P_m{}^{10}$ = 4160 Pa, which corresponds to the required parameters. It should be noted that providing the necessary setting time of the mixture required a certain increase in structural strength after 40 min of curing and other standardized strength values $P_m{}^{40}$ = 10,510 Pa, $f_{cm}{}^{3}$ = 17.2 MPa, $f_{cm}{}^{28}$ = 28.6 MPa and $f_{tn}{}^{28}$ = 8.7 MPa.

4. Values of the factors in natural form are determined by Equation (10):

$$\text{Bnd} = 0.9x_3 + 100 = 0.9 \times 100 + 400 = 490 \text{ kg/m}^3$$
$$\text{GBFS} = 0.62x_1 + 10 = 0.62 \times (-10) + 40 = 33.8\%$$
$$\text{HA} = 0x_2 + 1 = 0 \times 0 + 1 = 1\%$$

Calculated nominal composition of the cement–slag mixture without regard to water consumption:

$$\text{Bnd} = 490 \text{ kg/m}^3$$
$$\text{GBFS} = 490 \times 0.338 = 166 \text{ kg/m}^3$$
$$\text{Cem} = 490 - 166 = 324 \text{ kg/m}^3$$
$$\text{HA} = 0.01 \times 490 = 4.9 \text{ kg/m}^3$$
$$\text{SP} = 490 \times 0.003 = 1.47 \text{ kg/m}^3$$

The water content is determined by Equation (12):

$$W = 225 + 5 \times 0.62 - 4 \times 0 + 14 \times 0.9 + 2 \times 0.62^2 - 8 \times 0^2 - 4 \times 0.9^2 - 1 \times 0.62 \times 0.9 + 1 \times 0 \times 0.9 = 242 \text{ l/m}^3$$

5. Sand consumption from Equation (11):

$$A = \left(1000 - \left(\frac{324}{3.1} + \frac{166}{2.9} + \frac{242}{1}\right)\right) \times 2.65 = 1580 \text{ kg/m}^3$$

6. The value of the minimum possible cost of 1 m3 of mixture without taking into account the cost of water (found by iterating with the program application "Search for a solution"):

$$Ct_{cm} = 0.28 \times 324 + 0.02 \times 166 + 4.9 \times 2 + 1.47 \times 3.2 + 1580 \times 0.01 = 124.35\$$$

4. Conclusions

1. A set of mathematical models describing the effect of composition factors on the most important properties of fine-grained concrete mixture and concrete on cement–slag binder in the presence of hardening accelerator additive was obtained by using mathematical planning of experiments.
2. As a result of the analysis of the obtained models, the nature and quantitative estimates of the mutual influence of concrete composition factors on the studied properties were established. Composition factors were ranked depending on the intensity of their influence.
3. The relationships between structural strength and setting time, as well as various strength indicators of concrete produced on a 3D printer, were established for different values of mixture composition factors.
4. The use of a binder containing 30 ... 40% of ground-granulated blast-furnace slag and of hardening accelerator–sodium sulfate in the amount of 1 ... 2% by weight of the binder allows obtaining mixtures suitable for 3D printing.
5. The increased content of hardening accelerator–Na_2SO_4 leads to an increase in the compressive strength and splitting of concrete, as well as structural strength. An increase in the slag content of more than 40% is accompanied by a slight increase in

the water consumption of the mixture to ensure the required extrusion possibility and a decrease in strength.

6. Using mathematical programming implemented by Microsoft Excel and its "Search for a solution" application, the possibility of solving the problem of designing optimal compositions of construction mixtures used by a 3D printer was shown, based on the complex of experimental and statistical models.

Author Contributions: Conceptualization, L.D.; methodology, L.D. and V.M.; validation, L.D. and I.H., formal analysis, I.H. and M.M.; investigation, L.D. and V.M. resources, L.D., V.M., I.H. and M.M.; data curation, V.M.; writing—original draft preparation, L.D. and V.M.; writing—review and editing, I.H. and M.M.; visualization, V.M.; supervision, L.D. and I.H.; project administration, I.H.; funding acquisition, I.H. and L.D. All authors have read and agreed to the published version of the manuscript.

Funding: This work has been financed by the Polish National Agency for Academic Exchange under the International Academic Partnership Program within the framework of the grant: E-mobility and sustainable materials and technologies EMMAT (PPI/APM/2018/1/00027). The presented research was also supported by Polish Ministry of Science and Higher Education DWD/5/0237/2021.

Data Availability Statement: Not applicable.

Conflicts of Interest: The authors declare no conflict of interest. The funders had no role in the design of the study; in the collection, analyses, or interpretation of data; in the writing of the manuscript, or in the decision to publish the results.

References

1. Perrot, A.; Rangeard, D.; Courtaille, E. 3D printing of earth-based materials: Processing aspects. *Constr. Build. Mater.* **2018**, *172*, 670–676. [CrossRef]
2. Kaszynska, M.; Hoffmann, M.; Skibicki, S.; Zielinski, A.; Technan, M.; Olczyk, N.; Wroblewski, T. Evaluation of suitability for 3D printing of high performance concretes. In Proceedings of the MATBUD'2018—8th Scientific-Technical Conference on Material Problems in Civil Engineering, Szczecin, Poland, 15 June 2018; Volume 163. [CrossRef]
3. Ali, M.H.; Issayev, G.; Shehab, E.; Sarfraz, S. A critical review of 3D printing and digital manufacturing in construction engineering. *Rapid Prototyp. J.* **2022**. [CrossRef]
4. Xu, T.; Shen, W.; Lin, X.; Xie, Y.M. Additively manufactured thermoplastic polyurethane (TPU) mold for concrete casting of complex structure. *Rapid Prototyp. J.* **2022**. [CrossRef]
5. Khorasani, M.; Ghasemi, A.; Rolfe, B.; Gibson, I. Additive manufacturing a powerful tool for the aerospace industry. *Rapid Prototyp. J.* **2022**, *28*, 87–100. [CrossRef]
6. Le, T.T.; Austin, S.A.; Lim, S.; Buswell, R.A.; Gibb, A.G.F.; Thorne, T. Hardened properties of high-performance printing concrete. *Cem. Concr. Res.* **2012**, *42*, 558–566. [CrossRef]
7. Inozemtcev, A.S.; Korolev, E.V.; Duong, T.Q. Analiz suschestvuyuschikh tekhnologicheskikh resheniy 3D-pechati v stroitel'stve [Analysis of existing technological solutions of 3D-printing in construction]. *Vestn. MGSU* **2018**, *13*, 863–876. [CrossRef]
8. Perrot, A. (Ed.) *3D Printing of Concrete: State of the Art and Challenges of the Digital Construction Revolution*, 1st ed.; John Wiley & Sons Inc.: Hoboken, NJ, USA, 2019; 176p.
9. Ibrahim, M. Estimating the sustainability returns of recycling construction waste from building projects. *Sustain. Cities Soc.* **2016**, *23*, 78–93. [CrossRef]
10. Hager, I.; Golonka, A.; Putanowicz, R. 3D printing of buildings and building components as the future of sustainable construction. *Procedia Eng.* **2016**, *151*, 292–299. [CrossRef]
11. Chen, L.; He, Y.; Yang, Y.; Niu, S.; Ren, H. The research status and development trend of additive manufacturing technology. *Int. J. Adv. Manuf. Technol.* **2017**, *89*, 3651–3660. [CrossRef]
12. Secrieru, E.; Khodor, J.; Schrofl, C.; Mechtcherine, V. Formation of lubricating layer and flow type during pumping of cement-based materials. *Constr. Build. Mater.* **2018**, *178*, 507–517. [CrossRef]
13. Ma, G.; Buswell, R.; Leal da Silva, W.R.; Wang, L.; Xu, J.; Jones, S.Z. Technology readiness: A global snapshot of 3D concrete printing and the frontiers for development. *Cem. Concr. Res.* **2022**, *156*, 106774. [CrossRef]
14. Ilcan, H.; Sahin, O.; Kul, A.; Yildirim, G.; Sahmaran, M. Rheological properties and compressive strength of construction and demolition waste-based geopolymer mortars for 3D-Printing. *Constr. Build. Mater.* **2022**, *328*, 127114. [CrossRef]
15. Bolte, G.; Zajac, M.; Skocek, J.; Haha, M.B. Development of composite cements characterized by low environmental footprint. *J. Clean. Prod.* **2019**, *226*, 503–514. [CrossRef]
16. Miller, S.A.; John, V.M.; Pacca, S.A.; Horvath, A. Carbon dioxide reduction potential in the global cement industry by 2050. *Cem. Concr. Res.* **2018**, *114*, 115–124. [CrossRef]

17. Sanjuán, M.Á.; Estévez, E.; Argiz, C. Carbon Dioxide Absorption by Blast-Furnace Slag Mortars in Function of the Curing Intensity. *Energies* **2019**, *12*, 2346. [CrossRef]
18. Gruyaert, E.; Heede, P.; Belie, N. Carbonation of slag concrete: Effect of the cement replacement level and curing on the carbonation coefficient—Effect of carbonation on the pore structure. *Cem. Concr. Compos.* **2013**, *35*, 39–48. [CrossRef]
19. Dvorkin, L.; Dvorkin, O.; Ribakov, Y. *Mathematical Experiments Planning in Concrete Technology*; Nova Science Publishers: New York, NY, USA, 2011; 173p.
20. Dvorkin, L.; Bordiuzhenko, O.; Zhitkovsky, V.; Marchuk, V. Mathematical modeling of steel fiber reinforced concrete properties and selecting its effective composition. *IOP Conf. Ser. Mater. Sci. Eng.* **2019**, *708*, 012085. [CrossRef]